Effective index design of a shaped continuous unstable resonator for high power laser diodes

SALVADOR GUEL-SANDOVAL
Instituto de Investigación en Comunicación Óptica
Universidad Autónoma de San Luis Potosí
A. Obregón 64, 78000 San Luis Potosí, S.L.P., Mexico

ALAN H. PAXTON AND STEPHEN D. HERSEE
Center for High Technology Materials, University of New Mexico
Albuquerque NM, 87131-6081, USA

JOHN G. MCINERNEY
Department of Physics, University College Cork, Ireland

ABSTRACT. A geometric approach for a new type of unstable resonator, for high power and coherent semiconductor lasers, is described. The design is based on a theoretical model which predicts single mode operation for a wide waveguide with negative parabolic lateral effective refractive index (ERI) variation. A physical two waveguide model (or waveguide composed o two parts) is used to explain the functioning of such cavity. Radiation taking place in a primary high index region is directed by a secondary one where the optical intensity is lower. Analysis using the GRIN code shows only low order modes survive after multiple reflections.

RESUMEN. Se describe el diseño geométrico de un nuevo tipo de resonador inestable para láseres semiconductores de alta potencia. El diseño se basa en un modelo teórico, que predice operación monomodal, en una guía ancha de onda que contiene un índice de refración efectivo (IRE) lateral con variación parabólica negativa. Para explicar el funcionamiento de esta cavidad, se utiliza un modelo que supone dos guías de onda (o una guía de onda compuesta de dos partes). La radiación que tiene lugar en la región de índice de refracción alto, se desvía hacia otra región donde la intensidad óptica es menor. El análisis del diseño, usando el programa GRIN, demuestra que solamente los modos bajos sobreviven después de multiples reflexiones.

1. INTRODUCTION

Since its invention in 1962 the GaAs semiconductor laser has become a reliable and efficient miniature source of coherent light, calling immediately the attention of scientists and engineers to its multiple applications. Since then, modeling and then fabrication of new types of semiconductor laser have registered tremendous advances that are continuing through the 90's. The key to the expanding capabilities of semiconductors diode lasers

technology, has been the development of new structures, compounds, materials growth and fabrication techniques; in the continuing search for higher reliability and efficiency, better control and higher power operation [1].

The key area of research concerns two of the basic characteristics of a diode laser: the power obtained and the spatial coherence which determines the capability of the laser light to be focused. While many applications of diode lasers, such as optical pumping of solid state lasers, infrared laser illumination, laser soldering, eye surgery and others depend mainly on the level of power obtained from the laser, many others such as optical data storage, telecommunications via single mode fibers, satellite communication, printing, etc., require power and a high degree of spatial coherence at the same time.

Obtaining both high power and high spatial coherence simultaneously in a diode laser represents a difficult technical challenge, caused primarily by the spatial multimode behavior of the laser at high power levels. This insufficiency has resulted in much research work in the search for a laser design that includes both characteristics. Even though some methods have given satisfactory results, the search continues for better and more efficient laser structures and models.

Some of the most successful approaches to high power coherent laser diodes has been the phase-locked multichannel arrays [2–5] initiated by Scifres *et al.* in the late 70's, continued by Ackley and Engelmann [6,7] and by D. Botez *et al.* [8–10]; and master oscillator/power amplifier (MOPA) configurations [11–13], that consists of a master oscillator working at relatively low power, coupled to an amplifier that raises the power level.

Unstable resonators (URs) [14,15] have become another important approach. A UR cavity provides less amplification and increases the losses for the high order modes since they are spatially more extended and leave the cavity after a few passes. In contrast the fundamental (on-axis) mode stays in the cavity for more passes and therefore is amplified more. In this way discrimination in favor of the fundamental spatial mode, even for a large volume cavity, can be obtained [16].

Several UR cavity configurations are possible in a semiconductor laser. In 1980, Bogatov *et al.*, built an asymmetrical UR laser diode by grinding and polishing a cleaved facet into the shape of a curved surface, using diamond paste and a nylon string [17]. Even though the power level and the degree of spatial coherence reached were relatively low, this early work demonstrated the effectiveness of the UR method and encouraged the interest of many researchers.

In 1985 Craig *et al.* [18] and Salzman *et al.* [19], reported fabrication of similar UR diode lasers using wet chemical etching and reactive-ion-etching (RIE) techniques, respectively to etch curved mirrors on the facets of the laser. Later works by Largent *et al.* [20], Tilton *et al.* [21], and more recently DeFreez *et al.* [22], have shown the soundness of this approach by using improved techniques allowing more controllable parameters.

A different approach, that it is believed will lead to a more manufacturable device, consists in integrating the diverging elements inside the cavity by using a two part waveguide. The primary waveguide is an asymmetric graded-index and separate-confinement
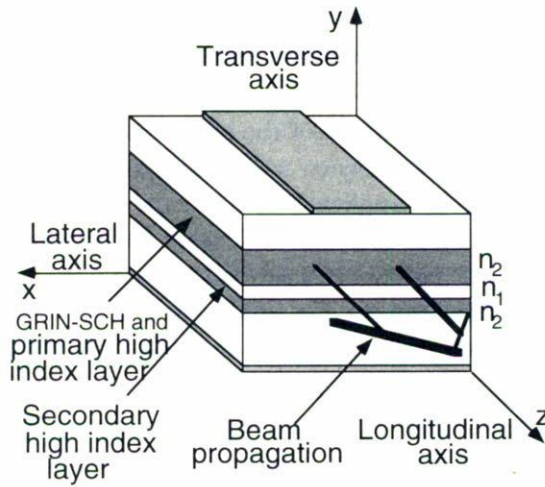
FIGURE 1. Illustrating the two part waveguide laser concept. Laser light is originated at the primary high index region. Lasing modes couple with the secondary high index region where diverging elements are incorporated that transform the medium into an unstable resonator.

laser heterostructure (GRIN-SCH) with a quantum well gain region. The lasing mode couples to a secondary waveguide located beneath or above the primary waveguide, where diverging elements are incorporated to provide the unstable resonator action. Figure 1 illustrates this idea.

One example of this is the regrown lens train (RLT) laser implemented by S.T. Srinivasan *et al.*, at the CHTM of UNM, in which negative diverging lens elements are etched into a GaAs layer above the GRIN-SCH and subsequently regrowth with a lower index p-type cladding layer [23].

The shaped unstable resonator (SHUR) laser (Fig. 2), is another approach using the same principle [24]. The SHUR laser is in some respects similar to the RLT laser, however light divergence is obtained in a different manner. Starting with an $Al_xGa_{1-x}As$ ($x = 0.4$, $n = 3.324$.)/GaAs ($n = 3.59$) GRIN-SCH, laser structure (Fig 3), an extra GaAs layer (etched layer), that has been previously photo etched with the aid of an almost parabolic Ar ion Laser beam, is located below the active layer. The two GaAs layers are embedded between two $Al_xGa_{1-x}As$ cladding layers [25]. This non-planar GaAs guide, designated as the etched layer (after the method used to fabricate it), causes an approximately parabolic lateral ERI variation of the medium, which is higher towards the sides of the structure as illustrated in the lower part of Fig. 2. So the optical cavity becomes a shaped unstable resonator (SHUR.)

The purpose of this work is to describe the geometrical design for such aforementioned SHUR laser cavity. The design is based on a theoretical model that predicts single mode operation, in a semiconductor laser, as long as radiation takes place in a medium with diverging index profile with quadratic variation in the lateral direction [26, 27].
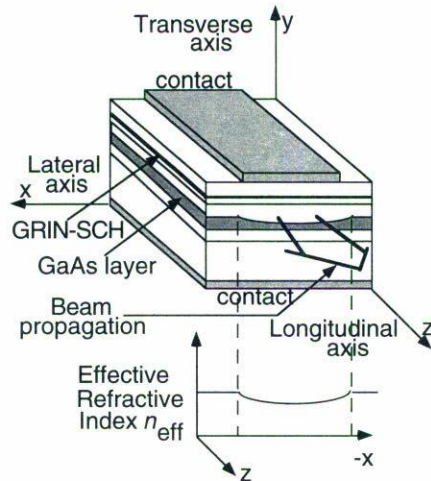
FIGURE 2. Schematic representation illustrating the SHUR laser concept. The curved area represents the photoetched GaAs layer (secondary waveguide) on top of which an $Al_xGa_{1-x}As$ layer is regrown and then the GRIN-SCH (primary waveguide) is completed. The medium becomes an unstable resonator after this operation due to the lateral effective index that increases with distance from the laser axis.
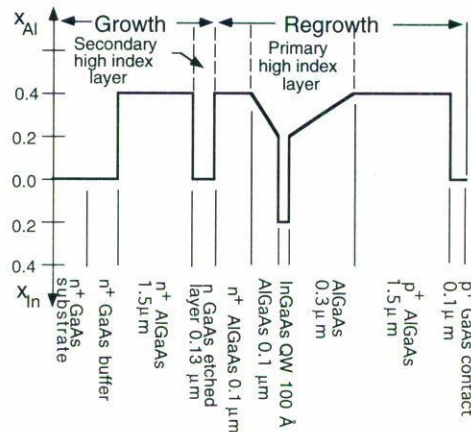
FIGURE 3. Transverse schematic view, not to scale, of the GRIN-SCH for the SHUR laser showing the variation of the composition. The structure is grown up to the GaAs layer and etched, then it is regrown until completed. A diagram of the refractive index variation along this direction can be seen in Fig. 9 when the GRIN code is used to graph the transverse mode.

2. GEOMETRIC THEORY OF SHUR CAVITY

When light propagates in a dielectric waveguide, a complex but interesting phenomenon occurs. Propagation takes place in modes, *i.e.*, not all directions in which light moves inside the slab are allowed. These modes are characterized by certain discrete values

of the light propagation constant in a given direction and depend on the real refractive indices and thicknesses of the layers forming the waveguide. Mathematically speaking, each mode is a solution to the wave equation in that medium and corresponds physically to a characteristic spatial distribution of the wave front.

If the medium is a waveguide formed by the superposition of several layers of different refractive index, which is the normal case for a diode laser, the layers interact in such a way that an ERI results for each mode [28]. This ERI ultimately determines the behavior of light inside the waveguide. Hence in general, light propagation can be affected by changes in the ERI of the waveguide medium.

If a lateral ERI variation is added to the waveguide such that the ERI increases with distance from the laser axis, the allowed modes will diverge as they pass along the cavity since, according to Snell's law, light always deviates towards the higher index regions. This leads to lateral anti-guiding.

If such a structurally modified medium is used as a resonant cavity for a semiconductor laser, where the light is bounced back and forth by the addition of facet mirrors at each end, this converts the medium into a continuous UR allowing coherent operation of a wide stripe laser at high power levels.

2.1. DESIGN OF THE SHUR CAVITY

For a basic understanding of the physics behind these fundamental ideas, it is essential to describe the optical properties of such continuous unstable cavity by deriving some useful formulas. Deduction of these formulas is done by using a geometrical optical approximation solution to the wave equation to determine the divergence path of laterally diverging light rays.

It can be proven [29] that for a medium whose index of refraction has a quadratic lateral dependence

$$n(x) = n_0 + n_2 x^2, \tag{1}$$

the light rays inside the medium are exponential curves described by

$$x = A e^{\eta z}, \tag{2}$$

as shown in Fig. 4; where x is the lateral direction, z is the beam propagation direction, n_0 is the refractive index at the center of the medium, n_2 is a constant (parabolic index profile) and η a constant that can be expressed as

$$\eta = \sqrt{\frac{2n_2}{n_0}}. \tag{3}$$

Also in such a case, the wavefronts are cylindrical, namely

$$S = n_0 z - n_0 \, a \, x^2, \tag{4}$$
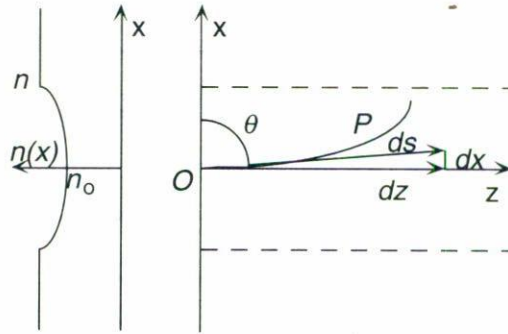
FIGURE 4. Propagation path P of light inside a one dimensional medium with quadratic lateral index variation.

where

$$a = \sqrt{\frac{n_2}{2n_0}} \tag{5}$$

and with a constant radius of curvature that is independent of the longitudinal coordinate z, given by

$$r = \frac{1}{2a} = \frac{1}{\eta} \, . \tag{6}$$

Also it is found that the laser magnification, defined as the lateral displacement of a ray at some position $x(z_0)$, divided by its value after a round trip propagation $x(z_0 + L)$, is expressed by

$$M = E^{e\eta L} \tag{7}$$

where L is the resonator length.

Equations (1)–(7) together with Figs. 5 and 6 are particularly useful in the design of the SHUR. Figure 5 is a schematic front view of the GaAs variable thickness etched layer showing the parameters used. In this figure d is the remaining thickness of the layer after etching, D is the maximum value allowed for d and n_D the ERI value at this point. At the center of the etching $x = 0$, $d = d_0$ and the ERI is equal to n_0. The etched depth is E_D and W is the maximum value of the etched profile width; while in Fig. 6, the lateral ERI for this structure has been calculated, as function of the GaAs layer etched depth d, with the aid of GRIN code.

To proceed with calculations, it is necessary to know the channel etched width W, the etched depth E_D and the length L of the laser. Values for M between $M = 2.6$ and $M = 7.3$ were used here as appropriate. Such values have been already mentioned for successful operation in other unstable resonators [29].

In general, suppose the values of n_0, M and L are fixed. From Eq. (1) the maximum value W of the etched width can be expressed in terms of n_D, n_0, and n_2 as

$$W = 2\sqrt{\frac{n_D - n_0}{n_2}} \, . \tag{8}$$
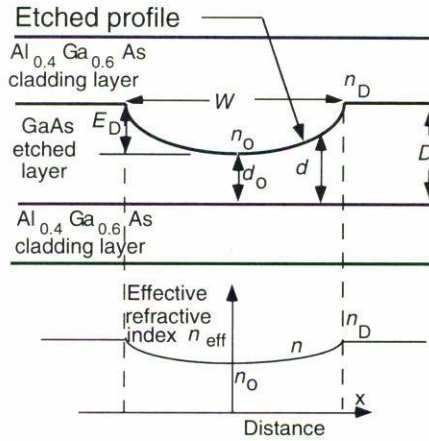
FIGURE 5. Schematic representation of the GaAs etching layer ($n = 3.59$) imbedded in the $Al_{0.4}Ga_{0.6}$ As cladding layer ($n = 3.324$), showing the basic parameters used for SHUR laser modeling. D is the unetched layer thickness, d_0 is the layer thickness at the center of the etching (at $x = 0$) and $n_{eff} = n_0$ at that point. At the edge of the etching (at $x = W/2$) $n_{eff} = n_D$. $E_D = D - d_0$ is the etched depth and W is the etched width. Lateral n_{eff} of the structure follows approximately the same variation as the etched profile.

Combining Eqs. (3) and (7) n_2 becomes

$$n_2 = \frac{n_0 \eta^2}{2} = \frac{n_0}{2} \left(\frac{\ln M}{2L} \right)^2. \tag{9}$$

Therefore for given values of n_0, M, and L, W depends only on the change in n from center to edge (this is: changes in n_D). Values of M can be also obtained as follows: suppose that the structure is etched so that $d_0 = 0.03$ μm at the center and $D = 0.13$ μm at the edge of the etched region (see Figs. 5 and 6), which automatically sets the etched depth $E_D = 0.1$ μm. If $W = 200$ μm, then the lateral distance x from the center to the edge of the etched region is 100 μm. It can be seen from Fig. 6 that $n = 3.3610$ (n_0) at the center and $n = 3.4063$ (n_D) at the edge of the etched width. From Eqs. (1), (3), and (7) we obtain $M = 5.165$, for $L = 500$ μm.

These results can be used to compare the SHUR design to other types of unstable resonator lasers, fabricated by other methods, through their equivalent geometrical properties. One may choose, for example, the same values for M that have been already set for reference ($M = 2.6$ and $M = 7.3$).

So for $L = 500$ μm and $n_0 = 3.3610$ and the corresponding values of n_2. The comparative expressions for W take the form:
For $M = 2.6$,

$$W = 2\sqrt{\frac{n_D - 3.3610}{1.534 \times 10^{-6} \ \mu m^{-2}}}.$$
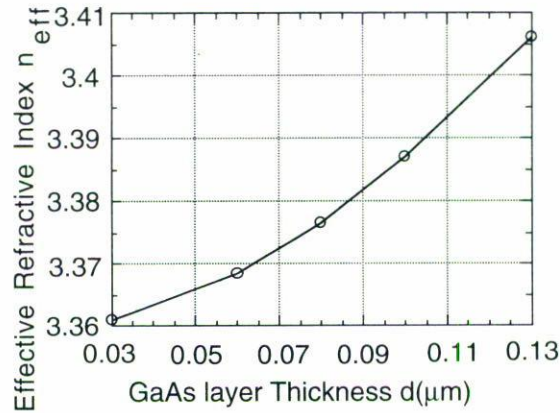
FIGURE 6. ERI variation as function of the GaAs etching layer thickness d, as given by the computer program GRIN. Total thickness etching layer D was 0.13 μm while d_0 was 0.03 μm.
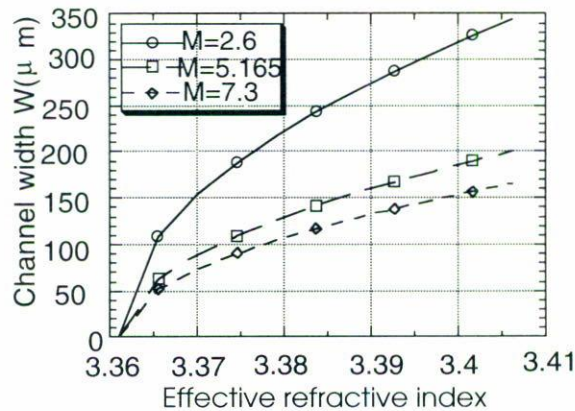
FIGURE 7. Etched channel width *versus* the effective refractive index of the medium for several typical values of laser magnification M.

For $M = 5.165$,

$$W = 2\sqrt{\frac{n_D - 3.3610}{4.530 \times 10^{-6} \ \mu\mathrm{m}^{-2}}}.$$

And finally for $M = 7.3$,

$$W = 2\sqrt{\frac{n_D - 3.3610}{6.640 \times 10^{-6} \ \mu\mathrm{m}^{-2}}}.$$

For these three different cases allowing n_D to vary between 3.3610 and 3.4063, which are the limit values as the etched layer thickness varies between 0.3 μm and 0.13 μm (Fig. 6), the graphs shown in Fig. 7 were obtained. So if a laser with $M = 2.6$ is desired, one choice is to set $W = 200$ μm and $n = 3.3765$ directly from the graph, which
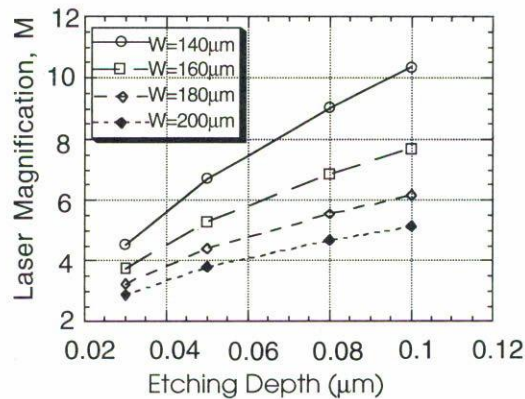
FIGURE 8. Laser magnification M as function of the etched depth, at different values of the channel width. Note the almost linear relationship among these variables. The etching layer total thickness D is 0.13 μm.

corresponds to an etching layer thickness of 0.08 μm and correspondingly to an etched depth of 0.05 μm. Hence a range of possibilities for simulating lasers with unstable resonators, by changing the etching conditions, are available.

Figure 8 shows a different case; the variation of the laser magnification M with the etched depth, for different etched widths. This graph allows the calculation of the value of M if the etching conditions are known. The relations are almost linear for the range of values used. Also note that this graph is valid only for refractive index values corresponding to GaAs and $Al_xGa_{1-x}As$ and would be somewhat different for different components.

From this graph it can be seen that etched depth values E_D between 0.030 μm and 0.080 μm together with an etched width channel $W = 160$ μm, would be appropriate to set typical M values between 2.6 and 7.3 (chosen previously as reference values for M). So this was the etching parameters range selected for the SHUR laser processing.

2.2. ANALYSIS OF THE ETCHED STRUCTURE WITH THE GRIN CODE

The GRIN computer code can be also used to calculate the amplitude distribution at the output of a laser structure where the number of layers, the thickness and refractive index of each one are known. The different layers are simulated simply by giving to the computer the real refractive indices and thicknesses of each layer. The results of the analysis help to establish the design of the actual resonator. This Section will show the results of the analysis done, with the GRIN computer code, to the modified GRIN-SCH structure.

Figures 9a to 9d show graphically the increased coupling that results from increasing the thickness d of the GaAs etching layer. These figures represent the optical field at various distances from the central axis in the lateral direction. It should be noted that the GRIN-SCH structure is asymmetric to assure adequate coupling of the exiting mode to the GaAs layer where mode discrimination takes place. Analysis shows the exiting
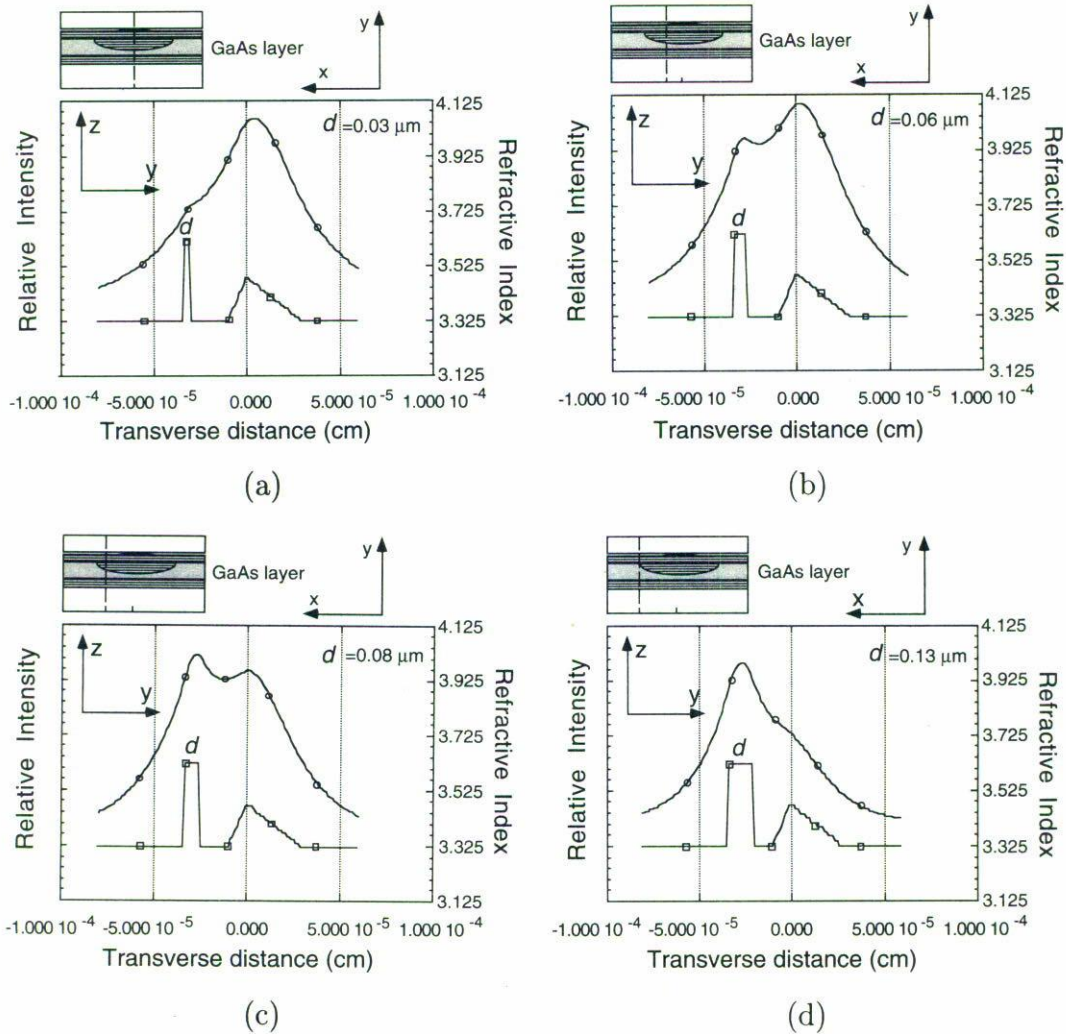
FIGURE 9. Schematic view of the SHUR laser structure different transversal planes showing the transverse refractive index variation (lower graph) and the outcoming optical field (upper graph), as simulated by the GRIN computer code. The top left figure is a front view of the laser structure. The dashed line indicates the mentioned plane. (a) Note at the center plane the GaAs etching layer thickness d is equal to 0.03 μm. (b) At a plane such that d is equal to 0.06 μm, note that the optical field starts being confined towards the sides of the structure. (c) At a plane where $d = 0.08$ μm, note that the optical field is still more confined into the etched channel. (d) Finally at a plane where $d = 0.13$ μm, note that the optical field is almost confined into the GaAs etching layer.

field amplitude distribution coupling from the primary to the secondary waveguide as the latter becomes wider and wider. At the center of the structure (Fig. 9a) light is mostly confined in the primary wave guide, while at the end of the etched section, light is concentrated at the secondary waveguide, as seen in Fig. 9d.

3. CONCLUSIONS

A key characteristic of the SHUR cavity is that gain discrimination depends almost exclusively on geometric factors that are determined by the etching conditions and are in principle flexible and manageable. This allows us to select the required value of divergence. In spite of the concept similarity between the RLT and the SHUR cavities, there is an important difference. The SHUR laser cavity contains none of the scattering interfaces that are present at each of the "lens" elements in the RLT device.

One important consideration, when designing the transverse structure, is to avoid supporting the second transverse mode, to guaranty suitable transverse spatial coherence. Previous modeling with the GRIN computer code showed that for values of d of less than 0.1 μm, only one mode exists inside the structure in the transverse direction [29]. For the SHUR cavity, this is the allowed range of values for the etching layer thickness to vary at the center of the structure (*i.e.*, $0.03 < d_0 < 0.1$ μm), to assure that only the fundamental transverse mode is excited.

Performance of SHUR laser devices fabricated by this method were described in detail in Ref. 24. However for the sake of comparison with other similar lasers, some of the data will be mentioned here: up to 770 mW pulsed, per facet, was obtained, with an external quantum slope efficiency of 66% double face. The threshold current was 1.4 A. A lobe of the focused beam, with twice the diffraction limited width, contained 47% of the single-facet power.

It should be mentioned that nature of light coupling among layers, as function of light polarization, wavelength and others parameters, was no studied. However such results could be included in a some different version of this work.

ACKNOWLEDGMENTS

REFERENCES

1. L. Figueroa (ed.), "High Power Laser Diodes and Applications," *Proc. SPIE* 893, (1988).
2. D.R. Scifres, R.D. Burnham, and W. Streifer, *Appl. Phys. Lett.* **33** (1978) 1015.
3. D.R. Scifres, W. Streifer, and R.D. Burnham, *Appl. Phys. Lett.* **34** (1979) 259.
4. D.R. Scifres, R.D. Burnham, and W. Streifer, *Appl. Phys. Lett.* **41** (1982) 118.
5. D.R. Scifres, R.D. Burnham, and W. Streifer, *Appl. Phys. Lett.* **41** (1982) 1030.
6. D.E. Ackley and R.W.H. Engelmann, *Appl. Phys. Lett.* **39** (1981) 27.
7. D.E. Ackley, *IEEE J. Quantum Electron.* **QE-18** (1982) 1910.
8. D. Botez *et al.*, *Appl. Phys. Lett.* **53** (1988) 464.
9. L.J. Mawst *et al.*, *Proc. SPIE* **1634** (1992) 2.
10. D. Botez, *IEE Proc. - J* **139** (1992) 14.

11. D. Mehuys, D.F. Welch, and L. Goldberg, *Electron. Lett.* **28** (1992) 1944.

12. R. Parke *et al.*, *IEEE Phot. Tech. Lett.* **5** (1993) 297.

13. R.J. Lang, S. O'Brien, D. Mehuys, and D.F. Welch, *Diode Laser Technology Program (DLTP)*, Sixth Annual Conference, 20-22 April 1993, Albuquerque NM, Sponsored by: Phillips Laboratory of the US Air Force.

14. A.E. Siegman, *Appl. Opt.* **13** (1974) 353.

15. H. Kogelnik and T. Li, *Proc. IEEE* **54** (1966) 1312.

16. A.E. Siegman, *Lasers*, Chapters 19 and 22, (University Science Books, Mill Valley CA, 1986).

17. A.P. Bogatov *et al.*, *Sov. J. Quantum Electron.* **10** (1980) 620.

18. R.R. Craig *et al.*, *Electron. Lett.* **21** (1985) 62.

19. J. Salzman *et al.*, *Appl. Phys. Lett.* **46** (1985) 218.

20. C. Largent *et al.*, *Proc. SPIE* **1418** (1991) 40.

21. M.L. Tilton *et al.*, *IEEE J. Quantum Electron.* **27** (1991) 2098.

22. R.K. DeFreez *et al.*, *Proc. SPIE* **1850** (1993) 75.

23. S.T. Srinivasan *et al.*, *Appl. Phys. Lett.* **61** (1992) 1272.

24. S. Guel-Sandoval, *et al.*, *Appl. Phys. Lett.* **66** (1995) 2048.

25. S. Guel-Sandoval *et al.*, (sent for publication).

26. M.L. Tilton, G.C. Dente, and A.H. Paxton, *SPIE Proc.* **1219**, Laser Technology and Applications II, (1990) 923.

27. A.K. Chan, C.P. Lai, and H.F. Taylor, *IEEE J. Quantum Electron.* **24** (1988) 489.

28. P. Yeh, *Optical Waves in Layered Media*, (Wiley & Sons, New York, 1988), Chapter 11.

29. A.H. Paxton, C.F. Schaus, and S.T. Srinivasan, *IEEE J. Quantum Electron.* **29** (1993) 2784.